ACS OMEGA

Open Access

http://pubs.acs.org/journal/acsodf

Article

Bidirectional Modulation on Electroporation Induced by Membrane Tension Under the Electric Field

Ping Ye, Lulu Huang, and Kuiwen Zhao*

Cite This: *ACS Omega* 2024, 9, 50458−50465

Read Online

ACCESS | Metrics & More | Article Recommendations | Supporting Information

ABSTRACT: Electroporation ablation is a minimally invasive nonthermal ablation technology that is applied to tumor ablation therapy. Given the varied morphologies of tumor cells, when an electric field is applied to the cell membrane surface, the direction of the electric field produces various angles with normal to the tangential plane of the cell membrane. In this study, we investigated the impact of cell morphology on membrane electroporation characteristics by adjusting the angle of the electric field relative to the cell membrane by using molecular dynamics simulations. The results show that the bidirectional modulation of cell membrane surface tension induced by Coulomb force can be triggered, allowing the electroporation effect to be regulated, by varying the angle between the electric field direction and the normal to the membrane. Electric field angles below 45° decreased phospholipid membrane surface tension, facilitating pore formation; angles above 45° enhanced the surface tension, elevating the energy barrier for pore opening and thus inhibiting pore formation. Furthermore, during the initial stage of membrane pore formation, water molecules penetrated the lipids, which aligned with the electric field and affected the pore tilt. The bidirectional modulation of the electric field in electroporation demonstrated that reversing the angle of the electric field is a potentially effective electroporation ablation protocol for improving the effectiveness of clinical cancer treatments.

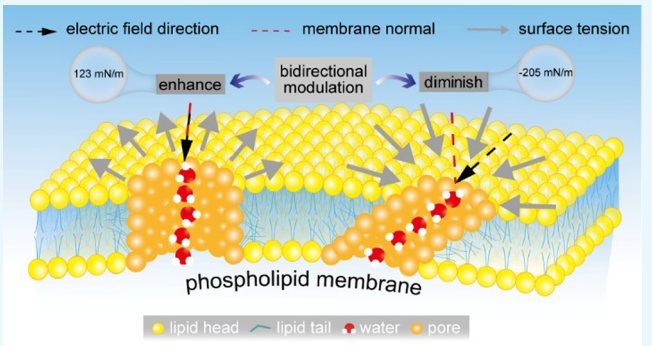

1. INTRODUCTION

Electroporation ablation has been proven to effectively treat multiple types of cancer.[1−4] Membrane electroporation can be broadly defined as a process in which the application of an external electric field to cells induces the rearrangement of membrane components, resulting in the formation of hydrophilic pores, thereby significantly enhancing the electrical conductivity and permeability of the plasma membrane.[5−7] The electroporation process, which involves the transition of the cell membrane from a sealed state to a porous state, occurs only in the vicinity of the applied electric field and lasts for microseconds.[8,9] Molecular dynamics simulations can provide detailed insights into the microscale behavior of cell membranes under the influence of electric fields. The electric field plays a crucial role in membrane electroporation, as the driving force for pore formation.

Cells typically exhibit various shapes and orientations.[10] Taking into account the varying curvatures of tumor cell membranes, when cells are exposed to an electric field, the direction of the electric field incident on the cell membrane intersects with the membrane normal vector at various angles, thereby influencing the electroporation properties of the membrane. Despite this, the direction of the applied electric field has been parallel to the normal vector of the phospholipid membrane surface in recent molecular dynamics simulation studies on electroporation of planar phospholipid membrane.[11−14] Polak et al.[15] reported that the threshold for membrane electroporation is related to the lateral pressure applied at the water/lipid interface, which hinders the local diffusion of water molecules into the hydrophobic core, thus reducing the likelihood of pore formation. Moreover, as MD simulations of intact cells are impractical, and the irregular shapes of cells lead to diverse angles between the electric field and the cell contact surface, this study investigated the influence of cell morphology on electroporation by varying the angle of the electric field relative to the normal vector of the phospholipid membrane. Through electrode configuration changes, researchers can modify the angle of the electric field relative to the ablation target in electroporation experiments. This is critical for understanding the mechanics of electroporation, optimizing the use of electroporation technology and exploring its potential biomedical applications.

Received: August 15, 2024
Revised: October 19, 2024
Accepted: December 6, 2024
Published: December 13, 2024

Here, we demonstrate the effect of cell morphology on the electroporation properties of the phospholipid membrane by adjusting the angle of the electric field relative to the cell membrane, using molecular dynamics simulations. This study found that by altering the angle between the electric field and the cell membrane, bidirectional modulation of membrane surface tension can be achieved: when the electric field angle was less than 45°, reduced membrane tension facilitated pore formation; whereas when the angle exceeded 45°, increased membrane tension made pore formation more difficult. Moreover, during the first phase of pore formation, water molecules first rushed into the hydrophobic area of the phospholipid molecules and aligned with the direction of the electric field. The tilt angle of the membrane pore formation progressively leaned toward the direction of the electric field owing to the hydrophilic interaction of the phospholipid head groups.

2. RESULTS

2.1. Equilibrium of Membrane Properties. The molecular model is shown in Figure 1a. Dark blue, white, and yellow particles represent the phospholipid membrane, and light blue and red particles represent polar water molecules and NaCl, respectively. The dimensions of the entire system were 17.3 × 17.3 × 12.5 nm. The density of bulk water was 1025 kg/m^3 (Figure 1b), which is in line with previous studies.[12] The peaks indicated that choline, phosphate, and glycerol of the phospholipid bilayer are symmetrically distributed around −1 and 1 nm along the *Z*-axis. This aligned with prior research finding.[16] The thickness of the phospholipid membrane was 4.336 nm, which is in agreement with the result of a previous study.[17] The density distribution of each component in System 1 (Figure S1) was similar to that of the system.

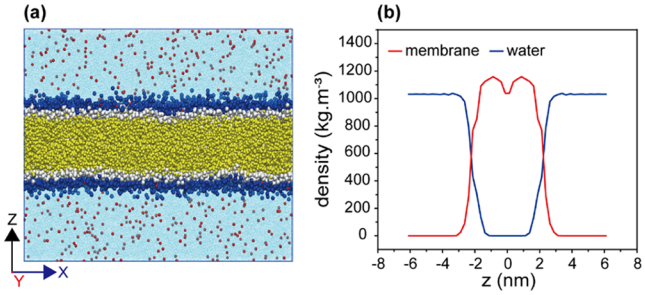

Figure 1. Balance-related indexes of the phospholipid membrane system. (a) Side view of the phospholipid membrane solution system. Dark blue, white, and yellow particles represent the DPPC phospholipid membrane, and the light blue and red particles represent polar water molecules and NaCl ions, respectively. (b) The density distribution of each component in the system. The membrane density represents the density of the entire phospholipid molecule, including choline, phosphate, glycerol, and fatty acids.

2.2. Inhibitory Effect of Electric Fields on Membrane Electroporation. In fact, during the cell electroporation process, the electric fields applied to the cell surface are not always perpendicular because of different cell morphologies. To further elucidate the role of the electric field orientation in the membrane electroporation characteristics, we investigated the effects of different electric field components on the phospholipid membrane by applying electric fields at various angles. An electric field was simultaneously applied along the positive directions of the x and z axes of the simulation box (with the normal of the phospholipid membrane parallel to the *z* axis of the simulation box) such that the resultant electric field of the two forms a fixed angle with the membrane normal vector. The electroporation in our simulations is irreversible. The pores do not close after the electric field is removed. Given that the Ex and Ey components of the electric field showed no difference in the characterization of pore formation, this study considered only Ex and Ez. Our results indicate that the larger the angle of the electric field, the more difficult it was for pores to form within a short period of time (Figure 2a). As the angle of the electric field increased from 0° to 50°, the time for pore formation was extended by 2 ns at 0.4 V/nm and by 0.6 ns at 0.5 V/nm. To avoid edge effects,[18] we conducted simulations with additional larger size molecular system. Under the influence of the resultant electric field of 0.5 V/nm at 50°, the pore formation times for both are approximate.

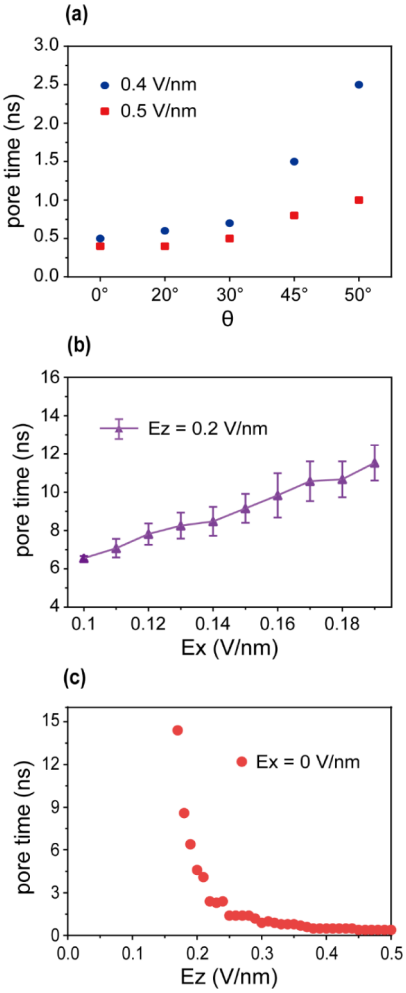

Figure 2. Influence of the electric field component on the pore formation time. (a) Change in the time of pore formation under different angles of the electric field (θ). (b) The change in trend of the pore formation time with Ex. (c) The pore formation time varies with the Ez.

To confirm that the increasing time for pore formation with the electric field angle was not due to the difference in the electric field strength in the Z direction (Ez), we further investigated the impact of the electric field angle on pore formation under the same Ez. A different electric field angle

https://doi.org/10.1021/acsomega.4c07396
ACS Omega 2024, 9, 50458−50465

was obtained by changing the electric field strength in the X direction (Ex). Here, we analyzed the effect of Ex on the pore formation time of the phospholipid membrane when Ez was maintained at 0.2 V/nm. The time required for pore formation was directly proportional to Ex. When Ex was increased from 0.1 to 0.19 V/nm, the time for membrane pore formation increased by a factor of 1.75 (Figure 2b). The electric field triggered the formation of membrane pores, with Ez accelerating pore formation and Ex impeding pore formation.

To evaluate the relationship between the electric field intensity parallel to the membrane normal vector and the pore formation time, the electric field of 0.15−0.5 V/nm was applied to the phospholipid membrane along its normal vector with a 0.01 V/nm interval. Consistent with the expected results, the membrane pore formation time decreased with an increasing electric field intensity (Figure 2c), and the size of the pores correspondingly increased (Figure 3a−d). Compared

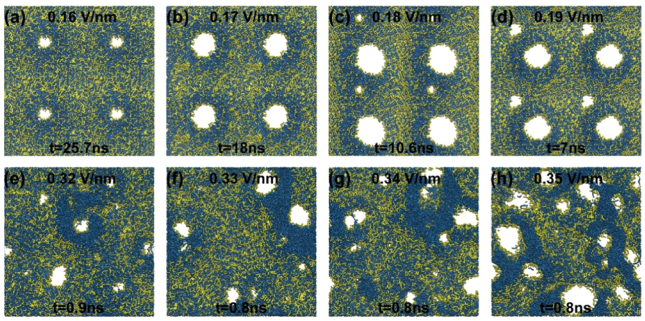

Figure 3. Snapshots of pore formation in phospholipid membrane with varying electric field intensities applied along the lipid phospholipid normal vector.

to lower electric fields, higher electric fields induced a greater number of membrane pores (from 6 pores at 0.32 V/nm to 15 pores at 0.35 V/nm) (Figure 3e−h). We estimated the pore formation based on the presence of continuous water molecular diffusion streams in the hydrophobic regions of the phospholipid membrane due to the variability and complexity of pore sizes and shapes.

2.3. Bidirectional Modulation of Membrane Surface Tension by Horizontal Electric Field Component. The Coulomb force acting on the phospholipid membrane is expected to play a crucial role in elucidating the inhibition and enhancement effects of electroporation in different directions of the electric field. To further quantify the impact of cell morphology on the characterization of membrane pores, we examined the effects of various electric field angles on the Coulomb force acting on the phospholipid membrane along the box's XYZ dimensions. The Coulomb force in the XY plane was obtained by computing the vector sum of the Coulomb force in the X and Y directions.

Similarly, as the angle of the electric field changed, a negative correlation was observed between the forces acting on the phospholipid membrane in the XY plane and in the Z dimension. At the resultant electric field of 0.5 V/nm, as the angle of the electric field increased from 0° to 60°, the Coulomb force experienced by the phospholipid membrane in the XY plane perpendicular to the membrane normal vector increased by 1.1×10^5 kJ/mol/nm (Figure 4a), whereas the Coulomb force in the Z dimension parallel to the membrane normal vector diminished by approximately 89% (Figure 4b). Under the resultant electric field of 0.4 V/nm, similar results were observed (Figure S2).

Figure 5 illustrates the variation in the angle between the direction of the electric field and the normal vector of the phospholipid membrane with a specific curvature under different electric field orientations. For example, in rod-shaped cells, cellular poles are positioned in regions of the membrane with higher negative curvature (i.e., near the central dashed line in Figure 5). When the electric field angle at the cell poles is 0°, the angle of the electric field in membrane regions away from the poles gradually increases. Due to the higher electric field intensity normal to phospholipid membrane at the poles compared to regions further away, the number of pores at the poles is more. This indicates that cell morphology has a significant effect on electroporation. Specifically, rod-shaped cells lack condensation effects away from the poles,[19] leading to more pronounced expansion of pores in these areas compared to the poles after pore opening. Notably, the horizontal component of the coulomb force, which is perpendicular to the membrane normal vector, increased dramatically with an increasing angle of the electric field. This force change in the phospholipid membrane hindered pore formation by enhancing the surface tension of the phospholipid membrane.

Calculating the surface tension[20] of the phospholipid membrane revealed that the angle of the electric field had a considerable bidirectional modulation on the membrane surface tension (Figure 6). At the electric field angle of 45°, the surface tension was close to that without the electric field applied.[21] The surface tension of the membrane at 0° is smaller

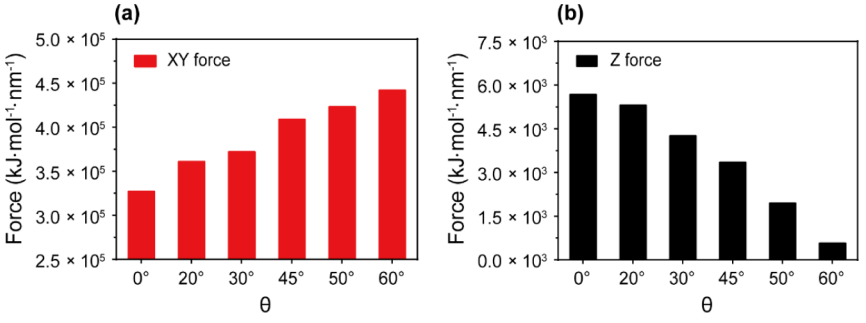

Figure 4. Coulomb force acted on the phospholipid membrane by an electric field with various angles (θ) (resultant electric field: 0.5 V/nm). (a) The Coulomb force of phospholipid membrane in the XY plane perpendicular to the membrane normal vector under different electric field angles θ. (b) The Coulomb force of phospholipid membrane in the Z dimension is parallel to the membrane normal vector under different electric field angles.

https://doi.org/10.1021/acsomega.4c07396
ACS Omega 2024, 9, 50458−50465

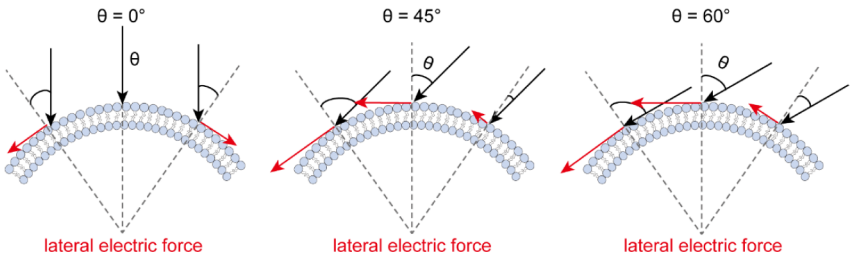

Figure 5. Variation of the lateral Coulomb force on the cell membrane surface under different electric field angles (θ). The dashed line in the phospholipid membrane is employed as a reference to determine the electric field angle. Here, the dashed line represents the membrane normal vector, the black arrow indicates the direction of the electric field, and the red arrow denotes the coulomb force exerted on the phospholipid membrane perpendicular to the membrane normal vector under the influence of the electric field, with the arrow length representing the magnitude of the force.

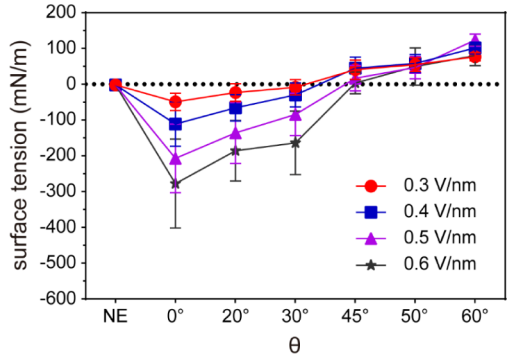

Figure 6. Surface tension of the phospholipid membrane induced by the electric field at various angles (θ). The red, blue, purple, and black lines represent the resultant electric field of 0.3 0.4, 0.5, and 0.6 V/nm, respectively. NE represents that without an electric field applied.

than that at 45°. The surface tension was markedly reduced when the electric field angle was below 45°, with higher fields more effectively reducing membrane surface tension than lower ones. In contrast, as the angle of the electric field exceeded 45°, surface tension increased significantly with the angle increased. It is worth noting that positive and negative surface tensions represented the relative change in membrane surface tension when compared with the state without the electric field. Negative values below 45° indicated a decrease in surface tension compared to the state without the electric field, which promoted pore formation. Positive values above 45° indicated an increase in surface tension, which prevented pore formation.

To investigate whether marangoni flow is induced in this research, we analyzed the density profile of water molecules in the XY plane near the phospholipid/solution interface (Figure S3). The results indicate that no obvious density difference is observed. According to previous study, marangoni flow is usually accompanied by pronounced density difference.[22] Thus, we inferred that there is no obvious marangoni flow in this research. Further comparison of surface tensions for membranes with different sizes showed that the surface tension is independent of the membrane size (Figure S4). Thus, we inferred that there is no obvious tension gradient in the plane of the membrane in this research.

Furthermore, we evaluated the diffusion coefficient of water molecules, and the findings revealed that the diffusion coefficient of water molecules dropped as the electric field angle increased (Figures S5). The permeability coefficient also dropped,[18] indicating that increasing the electric field angle prevents water molecules from penetrating the phospholipid layer, which is not conducive to pore formation.

2.4. Electric Field-Mediated Ordered Arrangement of Dipole Moments of Water Molecules. Interestingly, the snapshots (Figure 7a–d) show that when the angle of the

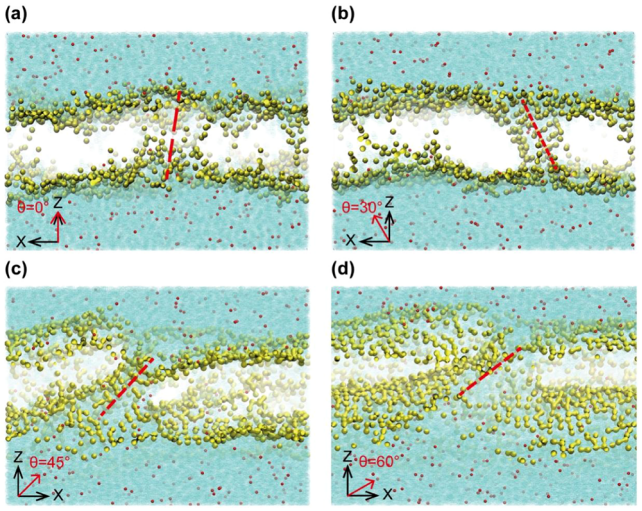

Figure 7. Snapshots of the pore characterization taken under various electric field angles (θ) in the projection of the system XZ plane. (a)–(d) Description the application of a 0.5 V/nm resultant electric field at angles of 0°, 30°, 45°, and 60°, respectively. The yellow particles represent the heads of phospholipid molecules, blue particles represent water molecules, and red particles represent NaCl ions. The pore axis is marked with a red dotted line.

electric field increased, the angle between the Z direction and the pore axis (the red dotted line) corresponded to the electric field direction. Under the resultant electric field of 0.4 V/nm, similar phenomena can also be observed (Figure S6a–Sd). This suggests that the electric field may also guide the alignment of pores along the direction of the electric field in addition to providing the energy required to induce membrane electroporation. This alignment along the electric field direction may be related to the orientation of the water molecules, which undergo an orderly arrangement under the influence of the electric field, thereby affecting the mechanism of pore formation.

Under the influence of an electric field, water molecules first penetrated the hydrophobic region of the phospholipid membrane, forming a chain of water molecules. Subsequently, the hydrophilic head groups of the phospholipid molecules interacted with the water molecules, inducing a rearrangement

https://doi.org/10.1021/acsomega.4c07396
ACS Omega 2024, 9, 50458–50465

of the phospholipids that led to the formation of a pore around the water chain, providing a passage for the water molecules to traverse the membrane (Figure 8a,b). This controlled remodeling of phospholipid molecules has a significant impact on the shape of the pores.

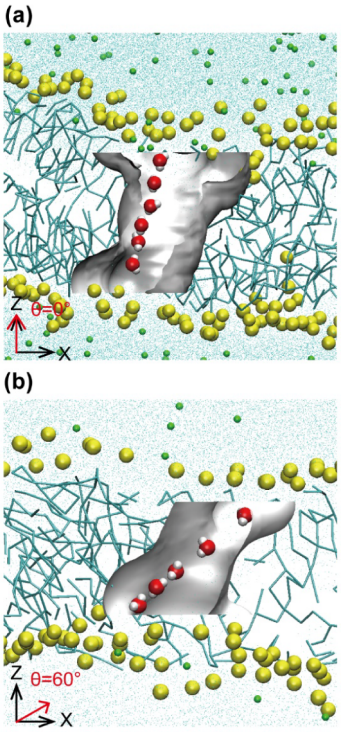

Figure 8. Snapshots of pore formation induced by water molecules invading the hydrophobic region at different electric field angles. (a), (b) depict the application of a 0.4 V/nm resultant electric field at angles of 0° and 60°, respectively. The gray and white areas represent the formed membrane pore, with the water molecules inside the pore depicted by red and white spheres; outside the pore, the phospholipid head, phospholipid tail, water molecules, and ions are represented, respectively, by yellow spheres, dark blue rods, light blue particles, and green spheres.

To validate the contribution of water molecules to the molding of pore shapes in the phospholipid membrane under the action of an electric field, we calculated the variation in the dipole moments of water molecules during the formation of membrane pores as a function of the electric field angle.[23,24] Although there were fluctuations in the orientation angle of the dipole moments of the water molecules in the XZ plane, they were mainly concentrated around the angle of the applied electric field (Figure 9a). When the system is subjected to an external electric field, the electric dipole moment of each water molecule is acted upon by a torque, resulting in a gradual alignment of its dipole moment with the direction of the electric field. The orientation of water molecules gradually aligned with the electric field direction while the external electric field persisted, thus modifying the configuration of the membrane pore. Furthermore, the average molecular dipole moment of water correlated positively with the intensity of the electric field (Figure 9b), similar to the case for the molecular box of pure water.[23] However, given the same electric field applied at different angles, the average total dipole moment of the water molecules remained significantly unchanged.

3. DISCUSSION

Here, we addressed the impact of cell morphology on the electroporation effect of the phospholipid membrane under a coarse-grained force field by varying the angle of the electric field, elucidating how the Coulombic force on the phospholipid membrane induced by different electric field angles modulates the formation of membrane pores through changes in membrane surface tension. Furthermore, the orientation of the electric field has a considerable impact on the variance in the dipole moments of the water molecules and plays an auxiliary role in the shaping process of the pore morphology.

The diverse shapes of tumor cells cause an unequal distribution of the electric field on the cell surface during cellular electroporation. To quantify the impact of cell morphology on membrane electroporation, this study investigated the manipulation of the electric field component on a planar membrane to achieve different angles between the electric field direction and the normal vector of the membrane. The components of the electric field parallel and perpendicular to the membrane normal vector exert antagonistic effects on the pore formation time as the angle of the electric field increased. Specifically, the enhancement of the electric field component perpendicular to the membrane normal vector inhibited the formation of pores, while the enhancement of the

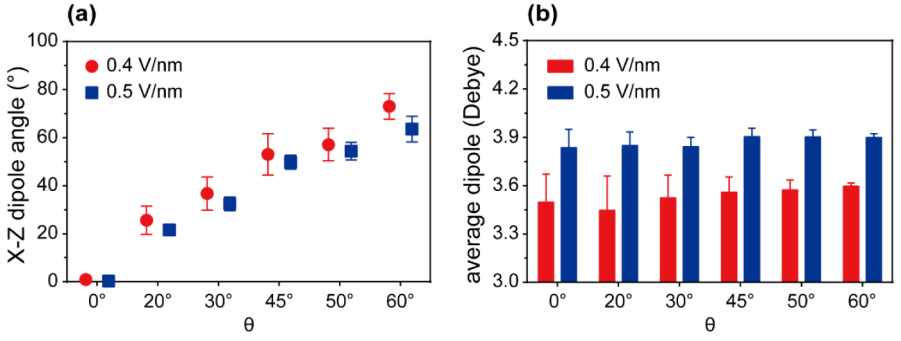

Figure 9. Dipole moment of water molecules changes with the angle of the electric field (θ). (a) illustrating the change in the total dipole moment of the water molecule under different electric fields and angles, where the blue, red, and green bars represent the applied resultant electric fields of 0.4 V/nm and 0.5 V/nm, respectively. (b) shows the relationship between electric field angle and dipole moment angle, with red and blue box plots denoting the applied resultant electric fields of 0.4 V/nm and 0.5 V/nm. The results were averaged over a 2 ns simulation period following formation of the pore.

https://doi.org/10.1021/acsomega.4c07396
ACS Omega 2024, 9, 50458−50465

electric field component parallel to the membrane normal vector accelerated the formation of pores (Figure 2a−c). This is consistent with the findings of Loche et al.,[25] which showed that the perpendicular response was decreased and the parallel dielectric response was greatly enhanced in the cephalic area of phospholipid membrane. This may be attributed to the fact that as the angle of the electric field increases, the reduction in the vertical component of the field diminishes the parallel dielectric response of water molecules, thereby limiting their migration toward the hydrophobic regions of the membrane,[26] establishing not favorable conditions for the emergence of pores.

Further force analysis revealed the mechanism by which variations in the angle of the electric field affected the electroporation effect of the phospholipid membrane. The formation of membrane pores is governed by the surface tension of the membrane.[27] With the application of electric fields at varying angles, the phospholipid membrane was subjected to an increased Coulomb force in the direction perpendicular to the membrane normal vector, while the Coulomb force parallel to the membrane normal vector was diminished. The cooperative effect of these two forces mitigates disturbances to the membrane, thereby further stabilizing the membrane structure and ultimately inhibiting the process of electroporation. Membrane tension, electric field intensity, and exposure duration all have an impact in electroporation, with higher tension requiring stronger fields and longer periods. Interestingly, the surface tension of the membrane exhibits bidirectional modulation as the electric field angle varies. In particular, electric field angles below 45° decrease the surface tension of the phospholipid membrane, reducing the energy needed to open the membrane pores. Angles above 45° increase the surface tension, raising the energy requirement for pore opening and inhibiting pore formation. Lateral pressure induced the transition from low-energy to high-energy molecular orientations, with increased surface tension correlating to a higher propensity for membrane rupture.[28] However, during electroporation of phospholipid bilayers, lipid molecules reorient from parallel to perpendicular to the membrane normal, resulting in hydrophilic transmembrane pores. This process was accompanied by an increase in membrane area, which causes a rise in surface free energy.[29] Consequently, the greater the electric-field-induced surface tension of the phospholipid membrane, the higher the difficulty in pore formation, necessitating a stronger electric field or prolonged exposure duration.

Clinically, the shape and size of the tumor can have an enormous effect on the penetration and distribution of the electric field, particularly when the tumor is large or irregularly shaped, which can result in inconsistent electroporation results.[30] When tumor ablation is ineffective after a number of electroporation sessions, the insertion angle of the ablation needle may be altered to improve the tumor ablation efficiency.

Furthermore, computational analysis of the water molecule dipole moments indicated that the electric field indirectly regulated the tilt angle of the membrane pores by modulating the orientation angle of the water molecule dipole moments. During the initial stage of pore formation, water molecules first permeate the hydrophobic region of the phospholipid membrane, followed by rearrangement of the phospholipid molecules. As described previously,[31] when subjected to an external electric field, the orientation of water molecule dipoles aligns with the direction of the applied field. The alignment of water molecule dipoles under various electric field orientations is not perfectly aligned due to the thermal motion.[32] Simultaneously, phospholipid molecules arrange themselves in an orderly manner around the water column, ultimately resulting in the tilt angle of the pore being similar to that of the electric field. These findings shed light on the regulatory effect of the electric field on the morphology of the membrane pores. The electric field has a direct impact on the alignment of water molecules, which in turn affects the reorganization of phospholipid molecules, modulating the membrane pore shape. Clinical research suggests that alterations in the pore morphology can affect the reparative capabilities of the cell membrane and the cellular viability. By modulating the electric field orientation, it is possible to regulate the morphology and dimensions of the pores, thus reducing harm to adjacent normal tissues to a maximum extent during therapeutic procedures and augmenting treatment safety.

4. CONCLUSIONS

In this study, we utilized coarse-grained molecular dynamics simulation techniques to uncover the properties of electroporation in phospholipid membranes in various cell morphologies. Our results demonstrate that the electric field angle regulates the occurrence of electroporation in the phospholipid membrane by modulating the Coulombic forces that act perpendicularly and parallel to the membrane normal. Notably, the surface tension of the phospholipid membrane is intimately associated with the forces exerted perpendicular to the membrane normal. It is noteworthy that the changes in surface tension of the phospholipid membrane under different electric field angles exhibit bidirectional modulation: Electric field angles of less than 45° diminish the surface tension of phospholipid membranes, favoring the formation of pores. Angles above 45°, conversely, increase the surface tension, raising the energy threshold for pore opening and thereby suppressing pore formation. Additionally, the directional changes in water molecule dipole moments under the influence of the electric field align with the angle of the electric field variation trends, exerting a pivotal influence on the modulation of the membrane pore morphology. This intricate dynamic balance offers a novel perspective for a profound comprehension of the effects of electric fields on the structural and functional aspects of phospholipid membranes. Although our study was unable to simulate the entire cell due to the computational limitations of MD simulations, the results are nonetheless informative for comprehending the impact of cell shape on the outcome of membrane electroporation.

These insights provide further understanding of the electroporation of cells and assist in optimizing the electroporation ablation strategy for cancer treatment to enhance therapeutic efficacy. Given the various forms of tumor cells, when an electric field is applied in a single direction, the angle formed at the cell surface varies with cell morphology. Altering the orientation of the ablation probe relative to the tissue to modify the angle of the electric field applied to the cell membrane is a potential strategy to improve the effectiveness of ablation procedures.

5. METHODS

The phospholipid membrane, composed of 1024-4096 DPPC molecules, was constructed by the CHARMMGUI membrane constructor.[33,34] The phospholipid membrane was immersed

https://doi.org/10.1021/acsomega.4c07396
ACS Omega 2024, 9, 50458−50465

in a 0.15 M NaCl solution, which is closest to the extracellular fluid of the body. The DPPC phospholipid membrane was experimentally characterized for membrane perforation, obtaining better sampling results for in vitro and in vivo experiments. All systems were simulated using the GROMACS simulation package[35] at coarse-grained (CG) resolution using the Martini force field.[11,12] Periodic boundary was applied at three directions.[36] This study established two models, with specific details provided in Supplementary Table SI. The leapfrog algorithm[14] was utilized in this MD simulation to integrate the equations of motion. The temperature was maintained at 310 K with the Berendsen[37] heat bath, and a pressure of 1 bar was maintained by the Parrinello−Rahman pressure coupling scheme[38] during the pre-equilibration process. This study applies the constant electric field with the duration of 50−200 ns and the intensity of 0.1−0.6 V/nm.[39−41] By modulating the range of values for the X components of the electric field (Ex) and the Z components of the electric field (Ez) (Table SII), the orientation of the resultant electric field (0.3 V/nm; 0.4 V/nm; 0.5 V/nm) was configured to form the angle (θ) with the normal vector of the phospholipid membrane, where θ was constrained between 0 and 60°. This study, building upon previous simulation researches,[12,39−42] applied the electric field intensity significantly exceeding experimental standards with the aim of observing significant membrane electroporation phenomena within the nanosecond-scale simulation time frame. The van der Waals force was smoothly switched to zero (between 1.0 and 1.2 nm), and electrostatic interactions were treated using the PME method.[43] All bonds involving hydrogen atoms were constrained using the LINCS algorithm.[44] All simulations utilized a 20 fs MD time step,[45] with each simulation run set to last 50 to 200 ns, and the coordinates were saved every 0.1 ns.

VMD[46] was used to generate all molecular images. The initial time of pore formation was determined by visually inspecting the generation time of the first water chain through the membrane in the hydrophobic layer of the phospholipid membrane.[47] The simulated trajectories were analyzed by using the built-in GROMACS analysis tool.

■ ASSOCIATED CONTENT

Data Availability Statement

Data used are available throughout the manuscript text.

Supporting Information

The Supporting Information is available free of charge at https://pubs.acs.org/doi/10.1021/acsomega.4c07396.

The electric field application protocol, the coulomb force experienced by the phospholipid membrane under a composite electric field of 0.4 V/nm, and snapshots of pore formation (PDF)

■ AUTHOR INFORMATION

Corresponding Author

Kuiwen Zhao − *School of Health Science and Engineering, University of Shanghai for Science and Technology, Shanghai 20093, China*; Email: kuiwenzhao@gmail.com

Authors

Ping Ye − *School of Health Science and Engineering, University of Shanghai for Science and Technology, Shanghai 20093, China*

Lulu Huang − *School of Health Science and Engineering, University of Shanghai for Science and Technology, Shanghai 20093, China*; orcid.org/0009-0007-1761-5481

Complete contact information is available at: https://pubs.acs.org/10.1021/acsomega.4c07396

Author Contributions

P.Y.: Conceptualization (equal); Writing—review and editing (equal); Supervision (equal). L. H.: Writing original draft-(equal); Data curation(equal); Visualization (equal). K.Z.: Conceptualization (equal); Methodology (equal); Writing—Review and Editing (equal).

Notes

The authors declare no competing financial interest.

■ ACKNOWLEDGMENTS

This research was financially supported by the Shanghai Co-Innovation Center for Energy Therapy of Tumors of China (No. 25) and Medicine-Engineering Interdisciplinary Project set up by University of Shanghai for Science and Technology, China.

■ REFERENCES

(1) Reddy, V. Y.; Dukkipati, S. R.; Neuzil, P.; Anic, A.; Petru, J.; Funasako, M.; Cochet, H.; Minami, K.; Breskovic, T.; Sikiric, I.; Sediva, L.; Chovanec, M.; Koruth, J.; Jais, P. Pulsed Field Ablation of Paroxysmal Atrial Fibrillation: 1-Year Outcomes of IMPULSE, PEFCAT, and PEFCAT II. *JACC Clin Electrophysiol.* **2021**, *7* (5), 614−627.

(2) Granata, V.; Fusco, R.; D'Alessio, V.; Giannini, A.; Setola, S. V.; Belli, A.; Palaia, R.; Petrillo, A.; Izzo, F. Electroporation-based treatments in minimally invasive percutaneous, laparoscopy and endoscopy procedures for treatment of deep-seated tumors. *Eur. Rev. Med. Pharmacol. Sci.* **2021**, *25* (9), 3536−3545.

(3) Shiomi, A.; Kaneko, T.; Nishikawa, K.; Tsuchida, A.; Isoshima, T.; Sato, M.; Toyooka, K.; Doi, K.; Nishikii, H.; Shintaku, H. High-throughput mechanical phenotyping and transcriptomics of single cells. *Nat. Commun.* **2024**, *15* (1), 3812.

(4) Gudvangen, E.; Kim, V.; Novickij, V.; Battista, F.; Pakhomov, A. G. Electroporation and cell killing by milli-to nanosecond pulses and avoiding neuromuscular stimulation in cancer ablation. *Sci. Rep.* **2022**, *12* (1), 1763.

(5) Anirudhan, T. S.; Nair, S. S. Development of voltage gated transdermal drug delivery platform to impose synergistic enhancement in skin permeation using electroporation and gold nanoparticle. *Mater. Sci. Eng.: C* **2019**, *102*, 437−446.

(6) Kotnik, T.; Rems, L.; Tarek, M.; Miklavčič, D. Membrane Electroporation and Electropermeabilization: Mechanisms and Models. *Annu. Rev. Biophys.* **2019**, *48*, 63−91.

(7) El-Kareem, S. A. A.; Hussein, N. G. A.; El-Kholey, S. M.; Elhelbawy, A. M. A. E. I. Microneedle combined with iontophoresis and electroporation for assisted transdermal delivery of goniothalamus macrophyllus for enhancement sonophotodynamic activated cancer therapy. *Sci. Rep.* **2024**, *14* (1), 7962.

(8) Vernier, P. T.; Levine, Z. A.; Wu, Y. H.; Joubert, V.; Ziegler, M. J.; Mir, L. M.; Tieleman, D. P. Electroporating fields target oxidatively damaged areas in the cell membrane. *PLoS One* **2009**, *4* (11), No. e7966.

(9) So, E. C.; Tsai, K. L.; Wu, F. T.; Hsu, M. C.; Wu, K. C.; Wu, S. N. Identification of minuscule inward currents as precursors to membrane electroporation-induced currents: real-time prediction of pore appearance. *Cell. Physiol. Biochem.* **2013**, *32* (2), 402−416.

(10) Towhidi, L.; Kotnik, T.; Pucihar, G.; Firoozabadi, S.; Mozdarani, H.; Miklavčič, D. Variability of the minimal transmembrane voltage resulting in detectable membrane electroporation. *Electromag. Biol. Med.* **2008**, *27* (4), 372−385.

(11) de Jong, D. H.; Singh, G.; Bennett, W. F.; Arnarez, C.; Wassenaar, T. A.; Schäfer, L. V.; Periole, X.; Tieleman, D. P.; Marrink, S. J. Improved Parameters for the Martini Coarse-Grained Protein Force Field. *J. Chem. Theory Comput.* **2013**, *9* (1), 687−697.
(12) Yesylevskyy, S. O.; Schäfer, L. V.; Sengupta, D.; Marrink, S. J. Polarizable water model for the coarse-grained MARTINI force field. *PloS Comput. Biol.* **2010**, *6* (6), No. e1000810.
(13) Hockney, R. W.; Goel, S.; Eastwood, J. Quiet high-resolution computer models of a plasma. *J. Comput. Phys.* **1974**, *14* (2), 148−158.
(14) Berendsen, H. Transport properties computed by linear response through weak coupling to a bath. In *Computer Simulation in Materials Science: Interatomic Potentials, Simulation Techniques and Applications*; Springer, 1991, pp. 139−155.
(15) Polak, A.; Bonhenry, D.; Dehez, F.; Kramar, P.; Miklavčič, D.; Tarek, M. On the electroporation thresholds of lipid bilayers: molecular dynamics simulation investigations. *J. Membr. Biol.* **2013**, *246* (11), 843−850.
(16) De Nicola, A.; Zhao, Y.; Kawakatsu, T.; Roccatano, D.; Milano, G. Hybrid Particle-Field Coarse-Grained Models for Biological Phospholipids. *J. Chem. Theory Comput.* **2011**, *7* (9), 2947−2962.
(17) Zhou, C.; Liu, K. Molecular dynamics simulation of reversible electroporation with Martini force field. *Biomed. Eng.* **2019**, *18* (1), 123.
(18) Zhao, K.; Wu, H. Size effects of pore density and solute size on water osmosis through nanoporous membrane. *J. Phys. Chem. B* **2012**, *116* (45), 13459−13466.
(19) Laloux, G.; Jacobs-Wagner, C. How do bacteria localize proteins to the cell pole? *J. Cell Sci.* **2014**, *127* (Pt 1), 11−19.
(20) Chen, F.; Smith, P. E. Theory and Computer Simulation of Solute Effects on the Surface Tension of Liquids. *J. Phys. Chem. B* **2008**, *112* (30), 8975−8984.
(21) Jähnig, F. What is the surface tension of a lipid bilayer membrane? *Biophys. J.* **1996**, *71* (3), 1348.
(22) Johansson, P.; Galliéro, G.; Legendre, D. How molecular effects affect solutal Marangoni flows. *Phys. Rev. Fluids* **2022**, *7* (6), 064202.
(23) Zhu, J. T.; Zhang, Z.; Ma, J. Electrostatic Interactions of Water in External Electric Field: Molecular Dynamics Simulations. *J. Electrochem.* **2017**, *23* (2), 207−216.
(24) Nymand, T. M.; Linse, P. Molecular dynamics simulations of polarizable water at different boundary conditions. *J. Chem. Phys.* **2000**, *112* (14), 6386−6395.
(25) Loche, P.; Ayaz, C.; Wolde-Kidan, A.; Schlaich, A.; Netz, R. R. Universal and Nonuniversal Aspects of Electrostatics in Aqueous Nanoconfinement. *J. Phys. Chem. B* **2020**, *124* (21), 4365−4371.
(26) Perrier, D. L.; Rems, L.; Kreutzer, M. T.; Boukany, P. E. The role of gel-phase domains in electroporation of vesicles. *Sci. Rep.* **2018**, *8* (1), 4758.
(27) Hasan, M.; Saha, S. K.; Yamazaki, M. Effect of membrane tension on transbilayer movement of lipids. *J. Chem. Phys.* **2018**, *148* (24), 245101.
(28) Agudelo, J.; Bossa, G. V.; May, S. Incorporation of Molecular Reorientation into Modeling Surface Pressure-Area Isotherms of Langmuir Monolayers. *Molecules* **2021**, *26* (14), 4372.
(29) Hu, Y.; Sinha, S. K.; Patel, S. Investigating Hydrophilic Pores in Model Lipid Bilayers Using Molecular Simulations: Correlating Bilayer Properties with Pore-Formation Thermodynamics. *Langmuir* **2015**, *31* (24), 6615−6631.
(30) Miklavcic, D.; Davalos, R. V. Electrochemotherapy (ECT) and irreversible electroporation (IRE) -advanced techniques for treating deep-seated tumors based on electroporation. *Biomed. Eng.* **2015**, *14* (Suppl 3), I1.
(31) Kasparyan, G.; Hub, J. S. Molecular simulations reveal the free energy landscape and transition state of membrane electroporation. *Phys. Rev. Lett.* **2024**, *132* (14), 148401.
(32) Zhao, K.; Wu, H. Structure-dependent water transport across nanopores of carbon nanotubes: toward selective gating upon temperature regulation. *Phys. Chem. Chem. Phys.* **2015**, *17* (16), 10343−10347.
(33) Jo, S.; Kim, T.; Iyer, V. G.; Im, W. CHARMM-GUI: a web-based graphical user interface for CHARMM. *J. Comput. Chem.* **2008**, *29* (11), 1859−1865.
(34) Wu, E. L.; Cheng, X.; Jo, S.; Rui, H.; Song, K. C.; Dávila-Contreras, E. M.; Qi, Y.; Lee, J.; Monje-Galvan, V.; Venable, R. M.; Klauda, J. B.; Im, W. CHARMM-GUI Membrane Builder toward realistic biological membrane simulations. *J. Comput. Chem.* **2014**, *35* (27), 1997−2004.
(35) Abraham, M. J.; Murtola, T.; Schulz, R.; Páll, S.; Smith, J. C.; Hess, B.; Lindahl, E. GROMACS: High performance molecular simulations through multi-level parallelism from laptops to supercomputers. *SoftwareX* **2015**, *1*, 19−25.
(36) Mou, Q.; Xu, M.; Deng, J.; Hu, N.; Yang, J. Studying the roles of salt ions in the pore init.iation and closure stages in the biomembrane electroporation. *APL Bioeng.* **2023**, *7* (2), 026103.
(37) Parrinello, M.; Rahman, A. Polymorphic transitions in single crystals: A new molecular dynamics method. *J. Appl. Phys.* **1981**, *52* (12), 7182−7190.
(38) Darden, T.; York, D.; Pedersen, L. Particle mesh Ewald: An N·log (N) method for Ewald sums in large systems. *J. Chem. Phys.* **1993**, *98* (12), 10089−10092.
(39) Tieleman, D. P.; Leontiadou, H.; Mark, A. E.; Marrink, S. J. Simulation of pore formation in lipid bilayers by mechanical stress and electric fields. *J. Am. Chem. Soc.* **2003**, *125* (21), 6382−6383.
(40) Guo, F.; Wang, J.; Zhou, J.; Qian, K.; Qu, H.; Liu, P.; Zhai, S. All-atom molecular dynamics simulations of the combined effects of different phospholipids and cholesterol content on electroporation. *RSC Adv.* **2022**, *12* (38), 24491−24500.
(41) Marracino, P.; Caramazza, L.; Montagna, M.; Ghahri, R.; D'Abramo, M.; Liberti, M.; Apollonio, F. Electric-driven membrane poration: A rationale for water role in the kinetics of pore formation. *Bioelectrochemistry* **2022**, *143*, 107987.
(42) Miyazaki, Y.; Okazaki, S.; Shinoda, W. pSPICA: A Coarse-Grained Force Field for Lipid Membranes Based on a Polar Water Model. *J. Chem. Theory Comput.* **2020**, *16* (1), 782−793.
(43) Hess, B.; Bekker, H.; Berendsen, H. J.; Fraaije, J. G. LINCS: A linear constraint solver for molecular simulations. *J. Comput. Chem.* **1997**, *18* (12), 1463−1472.
(44) Ho, M. C.; Levine, Z. A.; Vernier, P. T. Nanoscale, electric field-driven water bridges in vacuum gaps and lipid bilayers. *J. Membr. Biol.* **2013**, *246* (11), 793−801.
(45) Stix, R.; Tan, X.-F.; Bae, C.; Fernández-Mariño, A. I.; Swartz, K. J.; Faraldo-Gómez, J. D. Eukaryotic Kv channel Shaker inactivates through selectivity filter dilation rather than collapse. *Sci. Adv.* **2023**, *9* (49), No. eadj5539.
(46) Humphrey, W.; Dalke, A.; Schulten, K. VMD: Visual molecular dynamics. *J. Mol. Graphics* **1996**, *14* (1), 33−38.
(47) Sun, S. *Molecular dynamics simulations of phospholipids in water under external electric field*; Hong Kong University of Science and Technology: HongKong, China, 2011. https://hdl.handle.net/1783.1/7300.

https://doi.org/10.1021/acsomega.4c07396
ACS Omega 2024, 9, 50458−50465